EXAFS Study of the Inner Shell Structure in Copper(II) Complexes with Humic Substances

GREGORY V. KORSHIN,*,[†]
ANATOLY I. FRENKEL,[‡] AND
EDWARD A. STERN[§]

Department of Civil Engineering, University of Washington, Box 352700, Seattle, Washington 98195-2700, Materials Research Laboratory, University of Illinois at Urbana−Champaign, Urbana, Illinois 61801, and Physics Department, University of Washington, Box 351560, Seattle, Washington 98195-1560

The structure of humic substances (HS) and their complexes with metal cations is a matter of ongoing debate. In this paper, the structure of Cu^{2+}−HS complexes was studied by extended X-ray absorption fine structure spectroscopy (EXAFS). This method is highly sensitive to the local structure around the target (e.g., Cu^{2+} or other cations). The CuO_6 octahedron was used to model the inner complexation shell of the Cu^{2+}−HS complexes. The quality of the fit of the EXAFS data was tested using model systems (copper(II)−aqua and −salicylate complexes). On the basis of the dissimilarity of the EXAFS spectra for the Cu^{2+}−tetrahydrofurantetracarboxylic acid complex from those of the Cu^{2+}−HS complexes, it is concluded that complexation sites of HS are not likely to contain carboxylic groups attached to a furan ring. The Cu−O distances in all Cu^{2+}−HS complexes were shorter than those in aqua or salicylate complexes. The contraction of the Cu−O distance was especially prominent for the axial direction, and the distortion of the inner shell was much reduced. The mean-square disorder values for the axial Cu−O pairs in Cu^{2+}−HS complexes indicate that the axial oxygens are more tightly bound with the central cation than those in either aqua or salicylic complexes, possibly indicating six-dentate coordination of Cu^{2+} by HS.

Introduction

Humic substances (HS) are ubiquitous organic oligomers or polymers with molecular weights ranging from <1000 to >100 000 Da (*1, 2*). Hydroxy- and methoxy-substituted aromatic units and aromatic ketone sites (collectively termed phenolic or polyhydroxyaromatic moiety, PHA) and carboxylic sites seem to be responsible for many reactions of HS (*3−8*). Alternative models hypothesize that the structure of HS either is similar to that of polymaleic acid with diminished impact of aromatic carbon (*9−11*) or is characterized by clustered carboxylic groups associated with cyclic α-ester or α-ether structures rather than with PHA (*12, 13*).

Heterocyclic units formed by condensation of carbohydrates with amino acids have also been proposed to constitute the building blocks of HS associated with the metal complexation (*14−16*).

Similar to the riddle of the general HS structure, the nature of metal complexation sites in HS is uncertain. For example, the Cu^{2+}−HS system has been studied by a number of methods (*17−27*). The ligands engaged in the complexation reactions have been identified as predominantly carboxyls and phenolic groups associated with PHA; in some cases a contribution of amines is suspected (*19−21*). Salicylic (2-hydroxibenzoic) acid has been frequently used as a model compound to represent the structure of Cu^{2+}-binding sites in HS (*21−23, 26−29*). The only way to confirm the salicylate-type model or alternative attributions of the metal complexation sites in HS is to carry out precise measurements of the distances between the cation and surrounding atoms, establish their identities, and probe the structure of HS beyond the first complexation shell. However, metal−HS complexes do not form crystals usable for conventional X-ray diffraction (XRD). Diffuse X-ray scattering is suitable only for solutions with high concentrations of the target since intense nonspecific scatter of X-rays is always observed in solutions. This necessitates the use of high metal concentrations (*30*) while metal−HS complexes are typically found at trace concentrations. Attempts to concentrate them may cause losses and alter the relevant equilibria. Therefore, the applicability of these techniques for studies of metal−HS complexes in solutions is very limited.

Extended X-ray absorption fine structure spectroscopy (EXAFS) has several important advantages in studying local structures in dilute solutions. EXAFS is sensitive only to the short-range order (*31*) and can probe the structure of both crystalline and noncrystalline samples. EXAFS is sensitive to the local structure around specific species of interest, such as Cu^{2+} or other cations. This makes it possible to directly measure partial pair correlation functions around the targeted atoms in solution with a relatively small number of structural variables. With the recent development of EXAFS data analysis methods (e.g., UWXAFS (*32*) and FEFF (*33*) computer codes), it has become possible to decipher the local structure in complex materials with a thorough error analysis. In addition, X-ray absorption near edge structure (XANES) measured in the same experiment with EXAFS contains information about the binding energy and oxidation state of the selected element (*34*). EXAFS has been proven to work very well with solutions of metal complexes (*35, 36*). The method has been used to study the inner shell structure of metal−HS complexes (*14, 37−41*), but its full potential and limitations in the structural studies of HS have to be explored in more detail. An attempt to use this technique to elucidate the structure of metal complexation sites in HS is presented in this paper.

Materials and Methods

Two HS samples were used in the experiments. The hydrophobic acids fraction (HPOA) from Suwannee River natural organic matter was obtained by Jerry Leenheer at the US Geological Survey Laboratory in Boulder, CO, using the XAD-8 adsorption procedure (*42*). HS from Judy Reservoir (JRHS), the main potable water supply for the city of Mt. Vernon, WA, was isolated using adsorption on iron oxide coated sand (IOCS) (*43, 44*). The column size was 2 L and the flow rate was 400 mL/min. The concentration of dissolved organic carbon (DOC) in Judy Reservoir water was 3.6 mg/L. Prior to adsorption, the water was acidified with HCl to pH

* Corresponding author phone: (206)543-2394; fax: (206)685-9185; e-mail: korshin@u.washington.edu.
† Department of Civil Engineering, University of Washington.
‡ University of Illinois at Urbana−Champaign. Author's mailing address: Building 510 E, Brookhaven National Laboratory, Upton, NY 11973.
§ Physics Department, University of Washington.

3.8, aerated to strip carbon dioxide, and passed through a column packed with IOCS. Approximately 80% of the dissolved organic carbon was retained by this procedure. The adsorbed JRHS was eluted with sodium hydroxide followed by neutralization and freeze-drying.

Elemental analyses showed that HPOA and JRHS contained <0.7% of nitrogen and <0.3% of sulfur. Ash in HPOA was <3.5%. The concentration of iron in HPOA and JRHS solutions was <50 μg/L. ^{13}C CP-MAS NMR spectroscopy (a Chemagnetics CMX 200 MHz spectrometer at a spinning rate of 5000 Hz was used) showed that HPOA contained 26% aromatic and 12% carboxylic carbon while JRHS had 22% aromatic and 12% carboxylic carbon. In both samples the concentration of functional groups active in metal binding was high enough to anticipate strong complexation with metal Cu^{2+} at molar Cu/C ratios less than 0.1.

The DOC concentration in all HS-containing solutions for EXAFS was 1000 mg/L. The desired amount of metal was added as copper perchlorate. Its concentration in the stock solution was determined using a Jobin-Yvon Ultratrace JY-138 ICP-AE spectrometer. The concentration of copper in the HS-containing solutions was 0.0025 M, thus the molar ratio Cu/organic carbon as C was 0.03. This copper concentration is expected to be below the saturation level of strongly binding sites in HS (20–22). Samples for EXAFS measurement were prepared at pH 4.0 and 12.0, filtered through a 0.22 μm Nuclepore polycarbonate filter, left overnight at 4 °C, and filtered again. The filtration was repeated a third time immediately prior to EXAFS measurements. In the absence of HS and other complexing agents, $Cu(OH)_2$ precipitated at pH > 5.5. This was prevented by HS that apparently complexed the copper and prevented the formation of the hydroxo species. Model systems included a copper(II)–aqua complex and copper complexes with salicylic (Sal) and tetrahydrofuran-2r,3t,4t,5c-tetracarboxylic acid (THFTCA). The metal and ligand concentrations were 0.01 and 0.1 M, respectively. The metal concentration in solutions containing only the copper–aqua complex was 0.1 M. $[Cu(H_2O)_6]^{2+}$ and Cu^{2+}–THFTCA solutions were prepared only at pH 4.0 since THFTCA did not prevent precipitation of copper hydroxide at pH > 5.5. Calculations of copper speciation in solutions were done using MINEQL+ software (45). The stability constants were not available for the Cu^{2+}–THFTCA system but the measurements with a copper-selective electrode showed that >90% of copper cation was complexed at pH 4.0.

Synchrotron EXAFS Measurements. X-ray absorption measurements were performed at the X11-A beamline of the National Synchrotron Light Source at Brookhaven National Laboratory. The Si(111) double-crystal monochromator was used to vary X-ray energy from 200 eV below to 850 eV above the absorption K edge of Cu (8979 eV). The samples were measured in fluorescence mode by using a Stern–Heald ionization detector (46). A nickel filter (3 absorption lengths thick) and Soller-type slits were used to minimize the fluorescence background. A partially transparent gas ionization chamber was used to measure the incident X-ray intensity (I_0). To minimize harmonics, the monochromator crystals were detuned by about 25%. Custom-designed liquid sample holders with an exposed solution volume of 0.25 mL (dimensions 25 mm × 5 mm × 2 mm) were used. Data of 2–4 scans for the same sample were averaged to improve the signal/noise ratio. To correct for a small angular drift in the position of the monochromator crystals between the scans, the data sets were carefully compared and adjusted vs their absolute energy before the averaging. The adjustment vs absolute energy was done using the position of a very narrow glitch in the I_0 detector channel as a reference point.

Processing of EXAFS Data. Methods of processing and analysis of EXAFS data have been constantly developing since EXAFS phenomena were first theoretically explained by Stern et al. (47, 48). To extract the contribution from atoms that surround the central radiation-absorbing atom of a target element, an isolated-atom smooth background function $\mu_0(k)$, where k is the photoelectron wavenumber, is subtracted from the experimental absorption coefficient $\mu(k)$, and the resultant signal is normalized by the absorption edge step:

$$\chi(k) = (\mu(k) - \mu_0(k))/\Delta\mu_0(0) \qquad (1)$$

The background of all the data was removed using an AUTOBK program (32, 49) using the energy reference E_0 located in the middle of the edge jump. In the single-electron single-scattering approximation, the edge step normalized EXAFS signal $\chi(k)$ generated by a given shell of atoms could be written as

$$\chi(k) = \frac{NS_0^2}{kR^2}f(k)\exp(-2k^2\sigma^2)\sin(2kr + \delta(k)) \qquad (2)$$

where N is the coordination number of the shell of the same atomic species located at approximately the same distance from the central atom, R is the average distance to the shell, σ^2 is the mean-square deviation of this distance (i.e., both static and dynamic disorder), and S_0^2 is the many-body factor introduced to account for the shake-up and shake-off effects of the passive electrons (31). $f(k)$ and $\delta(k)$ represent the photoelectron backscattering amplitude and phase shifts, respectively. The magnitude of the Fourier transform (FT) of $k^2\chi(k)$ in the r space gives a qualitative representation of the effective radial pair distribution function of nearest neighbors to Cu.

Until recently, reliable structural information could be recovered from EXAFS data only for the nearest shell surrounding the target atom. With the development of novel theoretical methods of ab initio calculations of $f(k)$ and $\delta(k)$ functions, EXAFS analysis has been increasingly accepted as a structure-sensitive technique that allows accounting for contributions from the atoms beyond the first shell surrounding the target and taking advantage of multiple-scattering contributions to the EXAFS signal (50, 51). In this study, ab initio FEFF6 code (33) was used to generate the $f(k)$ and $\delta(k)$ functions for the absorbing atom in a model structure. Next, the experimental EXAFS spectrum was fitted with the theoretical EXAFS function (eq 2) using the UWXAFS package (32) that provides a nonlinear least-squares fitting. During the fitting procedure, the corrections to the reference energy (ΔE_0), Cu–O distances for the equatorial and axial oxygens (ΔR), and mean-square disorders of the distances (σ^2) were varied until the best fit was achieved. The estimates of the errors in the parameters were also calculated. The fitting was performed in the r space by Fourier transforming both the experimental data and FEFF theoretical function. The k^2 weighting factor and the Hanning window function defined between 2 and 9–10 Å^{-1}, depending on the data k range, were used in Fourier transforms. The number of relevant independent data points N_{idp} in the data was calculated using eq 3 (52):

$$N_{idp} = (2\Delta k\Delta r/\pi) + 2 \qquad (3)$$

where Δk and Δr are the data ranges in k and r spaces, respectively. Formula 3 implies that the number of fit variables P should be smaller than N_{idp}. To reduce the number of fit variables, the many-body factor S_0^2 was fixed at 0.9, that is, the middle of its most probable variation range (0.8–1.0). In our fits, the typical number of variables was 5, while the number of relevant independent data points was
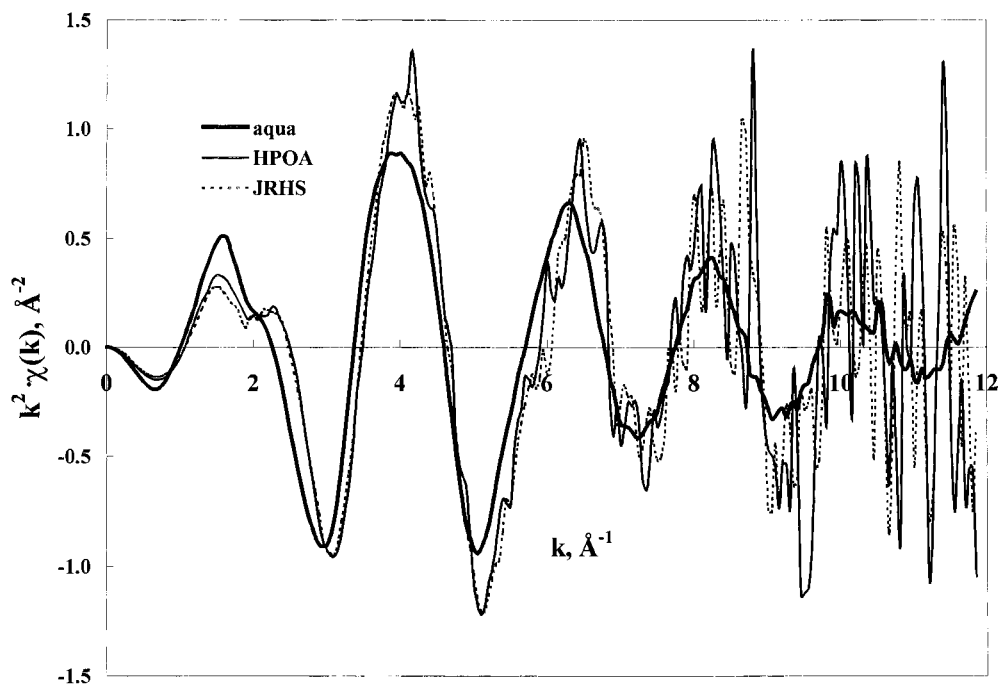
FIGURE 1. EXAFS spectra of solution containing copper(II)−aqua complexes and Cu^{2+}−HS) (pH 4). Copper concentration was 0.1 M for [Cu(H$_2$O)$_6$]$^{2+}$ and 0.0025 M for solutions containing Cu^{2+}−HS.

6−7, depending on the data range in k and r spaces. The possible impact of anharmonicity of the interatomic potentials was neglected due to the limited information in this regard. As discussed below, neglecting the anharmonicity does not affect our conclusions.

Results

Copper(II)−Aqua Complex. Similar to Palladino et al. (*53*), a CuO$_6$ octahedron was used to model the inner complexation shell in FEFF calculations for the aqua complex. Due to the axial distortion of the CuO$_6$ octahedron caused by the Jahn−Teller effect (*53, 54*), the distances between the central ion and the equatorial and axial oxygens were not identical. The initial estimates of the Cu−O distances were chosen based on a quantum chemical simulation that predicts the position of the two axial O atoms at 2.14 Å and the four equatorial oxygens at 2.0 Å from the central cation (*55*). The cluster used in FEFF calculations contained the central Cu atom and six water molecules surrounding it (four equatorial and two axial) in the first hydration shell. The distance between O and H atoms in water was 0.96 Å.

The normalized k^2-weighed EXAFS spectrum ($k^2\chi(k)$) for [Cu(H$_2$O)$_6$]$^{2+}$ is shown in Figure 1. The Fourier transform of the data for [Cu(H$_2$O)$_6$]$^{2+}$ is represented in Figure 2. Conspicuous maxima are seen at $r < 3.7$ Å while the absence of well-defined features for $r > 3.7$ Å is related to the large structural disorder beyond the first coordination shell surrounding the central cation. In fact, the water molecules beyond the first coordination shell were so disordered that their structural parameters could not be reliably determined by EXAFS. However, the contribution of the second hydration shell was included in the fit to evaluate the possible influence of these remote atoms on the EXAFS signal attributed to the atoms of the first hydration shell (between 1 and 2 Å). On the basis of the data of diffuse X-ray scattering (*30*), 11 oxygen atoms located at 3.95 Å from the central Cu^{2+} ion were used to represent the second hydration shell. The distribution of their positions was approximated with a Gaussian function. The impact of the second hydration shell into the EXAFS signal from the first shell was found to be negligible. Thus, the precision of the structural parameters of the first shell
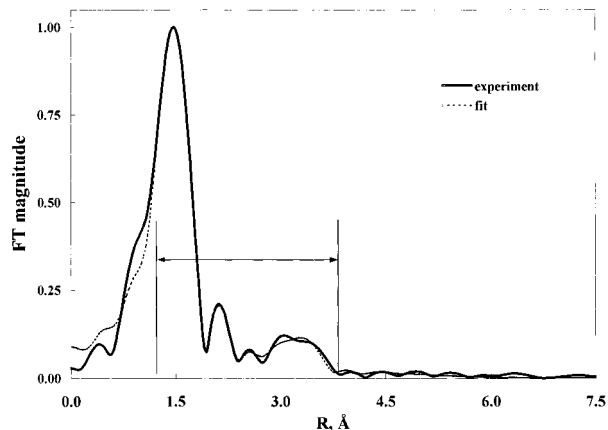

FIGURE 2. Fourier transform magnitudes of the EXAFS data and the best fit for the copper(II)−aqua complex. Copper concentration was 0.1 M. Arrow indicates the fitting range (1.2 to 3.8 Å).

determined by EXAFS is not affected by uncertainties of the structure of the more distant shells.

The Fourier transform magnitudes for [Cu(H$_2$O)$_6$]$^{2+}$ and the corresponding best fit are compared in Figure 2. The Cu−O distances and σ^2 derived from the fit are given in Table 1. The equatorial and axial Cu−O distances for [Cu(H$_2$O)$_6$]$^{2+}$ were found to be 1.97 ± 0.01 Å and 2.24 ± 0.03 Å, respectively. These results are practically identical with the EXAFS data for the copper−aqua complex reported in refs *36* and *56−59*.

Copper(II) Complexes with Salicylic Acid, THFTCA, and Humic Substances. The FT magnitudes of the $k^2\chi(k)$ data for copper(II) complexes with THFTCA, salicylic acid, HPOA, and JRHS at pH 4 are shown in Figure 3. In the range of $r < 1.8$ Å, these graphs are quite similar for the model compounds and Cu^{2+}−HS complexes. At $r > 1.8$ Å, the FT data for the Cu^{2+}-THFTCA system were very different from those generated for Cu^{2+} complexes with salicylic acid and HS. Due to the dissimilarity of the EXAFS spectra for the Cu^{2+}−THFTCA system at $r > 1.8$ Å, it is deduced that the complexation sites in HS are not likely to have furan-type

TABLE 1. Compilation of Structural Parameters Extracted from EXAFS Spectra for Copper(II) Complexes

| parameter	Cu–aqua, pH 4	Cu–Sal, pH 12	JRHS, pH 4	JRHS, pH 12	HPOA, pH 4	HPOA, pH 12
equatorial Cu–O, Å	1.97 ± 0.01	1.94 ± 0.01	1.93 ± 0.01	1.92 ± 0.01	1.92 ± 0.01	1.95 ± 0.01
axial Cu–O, Å	2.24 ± 0.03	2.20 ± 0.06	2.10 ± 0.02	2.13 ± 0.03	2.13 ± 0.02	2.14 ± 0.03
axial distortion, %	13.7 ± 2.1	13.4 ± 3.7	8.8 ± 1.6	10.9 ± 2.1	10.9 ± 1.6	9.7 ± 2.1
equatorial mean-square disorder Cu–O, Å^2	0.0049 ± 0.0002	0.0030 ± 0.0011	0.0046 ± 0.0016	0.0016 ± 0.0007	0.0000 ± 0.0016	0.0029 ± 0.0006
axial mean-square disorder Cu–O, Å^2	0.041 ± 0.020	0.023 ± 0.023	0.0065 ± 0.0052	0.0083 ± 0.0037	0.0011 ± 0.0047	0.017 ± 0.006
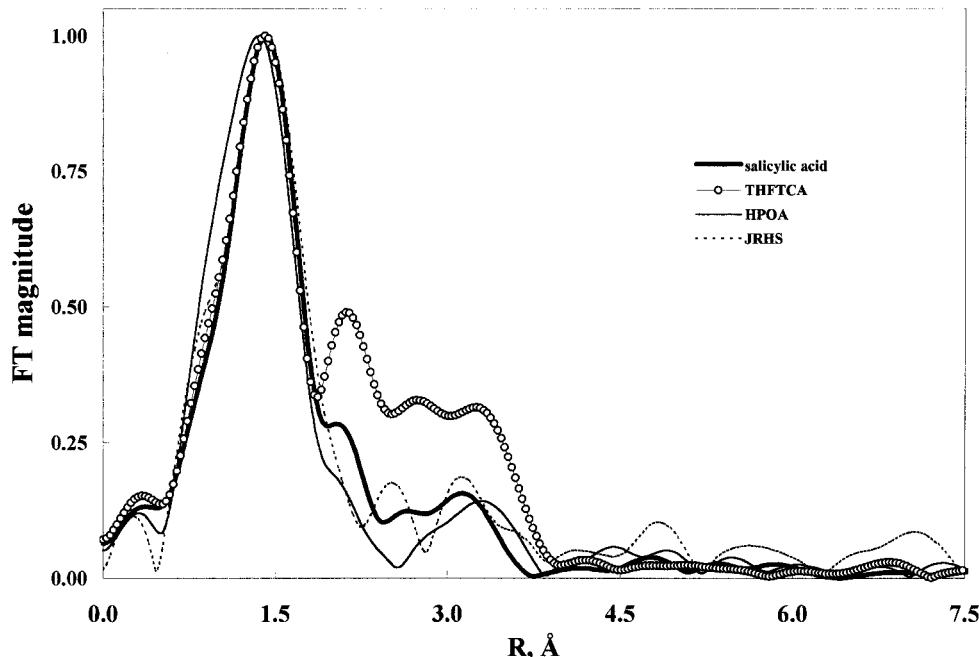
FIGURE 3. Fourier transform magnitudes of the experimental data of copper(II) complexes with model compounds and humic substances.

structures in the close vicinity of the complexed metallic cation.

Metal speciation calculations for the copper(II)−salicylic acid system showed that at pH 12 more than 99% of the copper exists as the $[Cu(Sal)_2(H_2O)_2]^{2-}$ complex while at pH 4 the $[CuSal(H_2O)_4]$ coexisted with an almost equal share of the copper−aqua complex. Since the presence of two species at pH 4 complicated the analysis, only the data for pH 12 were numerically processed. The FT magnitudes of the experimental $k^2\chi(k)$ data for copper(II)−salicylate system at pH 12 are shown in Figure 4. The fitting for this system was performed using the CuO$_6$ model with four oxygen atoms in the equatorial plane and two at the axial position. For FEFF calculations, the distances from the central Cu atom and the equatorial and axial O atoms in the $[Cu(Sal)_2(H_2O)_2]^{2-}$ complex were initially chosen from the quantum chemical calculations that yielded distances of 1.95 and 2.35 Å, respectively (55). The fit was made between 1.1 and 2.4 Å in r space (Figure 4), which corresponds to the first complexation shell. As demonstrated by the calculations for the aqua complex, the structural parameters obtained for the first shell are not affected by the subsequent shells. The best fit for the equatorial and axial Cu−O distances for the $[Cu(Sal)_2(H_2O)_2]^{2-}$ complex yielded 1.94 ± 0.01 and 2.20 ± 0.06 Å, respectively (Table 1). Both the equatorial and axial r_{Cu-O} values for this complex are shorter than those for $[Cu(H_2O)_6]^{2+}$, but the axial distortion, defined as $(r_{axial} - r_{equatorial})/r_{equatorial}$, is practically the same for $[Cu(H_2O)_6]^{2+}$ and $[Cu(Sal)_2(H_2O)_2]^{2-}$ complexes ($13.7 \pm 2.1\%$ and $13.4 \pm 3.7\%$, respectively).

Normalized k^2-weighed EXAFS spectra ($k^2\chi(k)$) for solutions containing Cu^{2+}−HS complexes are shown in Figure 1.
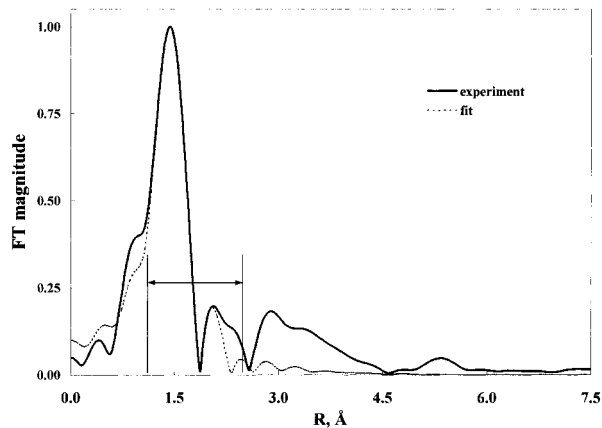

FIGURE 4. Fourier transform magnitudes of the data and fit for the copper(II)−salicylic acid system (pH 12). Metal concentration was 0.01 M, ligand concentration 0.1 M. Arrow indicates the fitting range (1.1−2.5 Å).

Due to the low concentration of copper in the HS-containing solutions (0.0025 M), substantial noise was observed for $k >$ 8 Å^{-1}. This could have been circumvented by increasing the concentration of copper in solution or by freeze-drying them, as was done by Xia et al. (40, 41). It was decided to maintain the metal concentration low in HS-containing solutions in order to be realistically close to natural environmental conditions and to explore the performance of EXAFS at these potentially challenging conditions. The high-frequency noise in the data at high k-range (>8 Å^{-1}) was predominantly
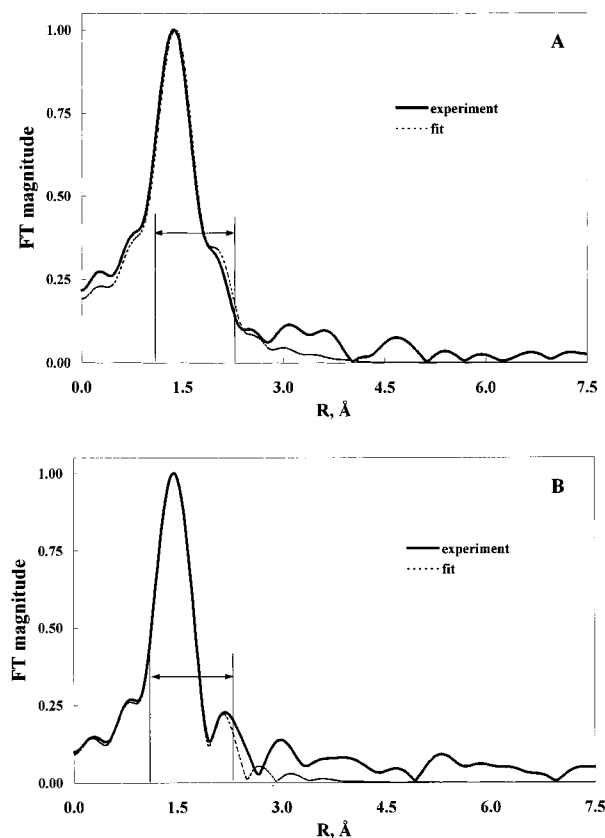
FIGURE 5. Fourier transform magnitude of the data and fit for the copper(II)−HPOA system at (A) pH 4.0 and (B) pH 12. Copper concentration was 0.0025 M, ligand concentration 1000 mg/L as C. Arrow indicates the fitting range (1.1−2.3 Å).

statistical and did not impair the data for the range of distances corresponding to the first complexation shell.

The data for Cu^{2+}−HS complexes differed from those for the copper−salicylate system. The FT magnitudes for the copper(II)−HPOA system are shown in parts A and B of Figure 5 for pH 4 and 12, respectively. The fitting was carried out for the range 1.1 Å $< r <$ 2.3 Å covering only the first coordination shell. On the basis of the very low concentration of nitrogen and sulfur in our samples (<0.7 and 0.3%, respectively), it was assumed that nitrogen and/or sulfur atoms were not present in the first complexation shell of the Cu^{2+}−HS complexes. For sulfur, this assumption is further supported by the fact that sulfur in aquatic HS is predominantly found in sulfonic groups which typically have low complexation activity (*60*). For nitrogen, the maximum molar Cu/N ratio was ca. 2.5. If all this nitrogen enters the complexation shell and the hydration number of Cu^{2+} is 6, only 1 per 15 water molecules in the Cu^{2+} hydration shell will be replaced and the impact of nitrogen in the first complexation shell in the EXAFS spectrum of Cu^{2+} will be <7%. The actual influence of nitrogen on the EXAFS spectra may be even less due to the competition between overwhelmingly abundant carboxylic groups and much less numerous amino groups. Thus, the EXAFS spectra of Cu^{2+}−HS complexes are expected to be absolutely predominated by oxygen-containing functionalities. Additional studies of the complexation shells other than CuO_6 (e.g., CuO_5N, CuO_4N_2, etc.) at varying Cu/N ratios using nitrogen-rich samples of HS are attractive, but this goal lies outside the scope of this paper.

Discussion

The data presented in Table 1 show substantially different axial and equatorial Cu−O distances and values of mean-square disorder (σ^2) for the model systems and Cu^{2+}−HS complexes. This permits us to infer important conclusions regarding the nature of the inner complexation shell in complexes of copper(II) with HS.

The dissimilar σ^2 values for the equatorial and axial Cu−O bonds in $[Cu(H_2O)_6]^{2+}$ reflect different strengths of interactions along these directions. The position of the equatorial oxygens vs the central cation is well defined and only small fluctuations of $r_{equatorial}$ are observed ($\sigma^2 = 0.0049 \pm 0.0002$ Å²). By contrast, the axial oxygens noticeably fluctuate around their averaged position ($\sigma^2 = 0.041 \pm 0.020$ Å²), which is almost 1 order of magnitude larger than that for the equatorial position. This result reflects the physics of Cu−O interactions. In the classical limit, i.e., for temperatures above the characteristic Einstein temperature, the value of σ^2 is inversely proportional to the force constant k: $\sigma^2 = k_B T/k$ (*31*). Correspondingly, the σ^2 data indicate that for the aqua complex the force constant k for the equatorial water molecules is 1 order of magnitude larger than that of the axial water molecules.

The axial and radial Cu−O distances for $[Cu(Sal)_2(H_2O)_2]^{2-}$ are somewhat shorter than those for the aqua complex, thus indicating an increased energy of Cu−O interactions. However, similar to the aqua complex, the σ^2 values for the equatorial and axial Cu−O bonds in $[Cu(Sal)_2(H_2O)_2]^{2-}$ are still markedly different for these two directions (0.0030 ± 0.0011 and 0.023 ± 0.023 Å², respectively), that is, the fluctuations of the water molecules along the z axis in $[Cu(Sal)_2(H_2O)_2]^{2-}$ are almost 1 order of magnitude more pronounced compared with those of the equatorial oxygens.

This is not observed for copper(II) complexes with HS. The equatorial Cu−O distances in Cu^{2+}−HS complexes at pH 4 and 12 are only marginally shorter than that for the $[Cu(Sal)_2(H_2O)_2]^{2-}$ complex, but the axial Cu−O distances are substantially decreased (2.10 to 2.14 and 2.20 Å for Cu^{2+}−HS and Cu^{2+}−Sal, respectively). The axial distortion of the HS complexes (8.8 to 10.9%) is less prominent than that of either $[Cu(H_2O)_6]^{2+}$ or $[Cu(Sal)_2(H_2O)_2]^{2-}$ (13.7 and 13.4%, respectively). It is also conspicuous that the σ^2 of the Cu−O pairs for the axial oxygens in Cu^{2+}−HS complexes is much smaller than that observed for aqua or salicylic complexes. That is, the axial oxygens are more steadily positioned vs the central cation in the complexes Cu^{2+}−HS compared with other studied systems.

This appears to indicate that the complexation mechanism in HS includes the formation of bonds along both the equatorial and axial directions. Otherwise, the contraction of the axial Cu−O distance and well-defined position of the axial oxygens vs the central cation (that is, the low corresponding σ^2 value) cannot be explained. That is, the axial oxygens in the Cu^{2+}−HS complex are likely to belong to an organic molecule rather than to water molecules. The number of HS molecules participating in complexation with the central Cu^{2+} cation is not certain, but due to a relatively large size of the HS molecules, the inclusion of more that one HS molecule into the inner complexation shell is not very likely. Thus, six-dentate complexation of copper by the binding site in HS may be inferred. This may not be simulated by salicylic acid or its derivatives, and the chemical nature of the HS complexation sites needs to be further ascertained.

The marked difference between the inner shell structure in the HS complexes and that of either $[Cu(H_2O)_6]^{2+}$ or $[Cu(Sal)_2(H_2O)_2]^{2-}$ is not an artifact of our fitting procedure in which the anharmonic correction to the Gaussian pair distribution function was neglected. It is well known that

neglecting the correction for anharmonicity causes the apparent interatomic distances derived from the fit to decrease (*31*). However, the impact of anharmonicity on the bonds with small disorder σ^2 is expected to be small. For the $Cu^{2+}-HS$ complexes, the correction for anharmonicity is expected to be negligible both for axial and equatorial $Cu-O$ distances since their σ^2 are also relatively small. For $[Cu(H_2O)_6]^{2+}$ or $[Cu(Sal)_2(H_2O)_2]^{2-}$, the correction for anharmonicity is insignificant for the equatorial $Cu-O$ distances for which the σ^2 values were also small but it would affect the more disordered axial $Cu-O$ bonds in $[Cu(H_2O)_6]^{2+}$ or $[Cu(Sal)_2(H_2O)_2]^{2-}$, possibly causing the corrected axial $Cu-O$ distance in these complexes to be somewhat larger than that obtained in this work. Thus, our results for the axial distortions for $[Cu(H_2O)_6]^{2+}$ and $[Cu(Sal)_2(H_2O)_2]^{2-}$ provides its lower limit. This reinforces our conclusion that the inner shell structures in the HS complexes and model systems are different above experimental uncertainties.

Data from independent EXAFS studies largely corroborate our conclusions regarding the nature of the copper-binding sites in HS. The average r_{CuO} distance in $Cu^{2+}-HS$ complexes was reported as 1.95–1.96 by Xia et al. (*40, 41*) and 1.92–1.93 Å by Herstberg et al. (*37*). The distortion of the CuO_6 octahedron in $Cu^{2+}-HS$ complexes determined by Xia et al. (*40, 41*) ranged from 1.5 to 4.7%. We observed a more prominent distortion of the CuO_6 structure in $Cu^{2+}-HS$ complexes (8.8–10.7%), but in both cases it was substantially less than that in the aqua or salicylic acid complexes (ca. 13.7%). However, liquid samples were used in our experiments while freeze-dried specimens were analyzed by Xia et al. (*40, 41*), so direct comparison of the corresponding results is unreliable.

The issue of axial distortion in $Cu^{2+}-HS$ complexes was not addressed by Hersterberg et al. (*37*), and the average $Cu-O$ distances reported in that work appear to be significantly underestimated. Even for a model system containing 0.005 M copper acetate at pH 6 where copper(II)–aqua complexes should predominate, the reported average $Cu-O$ distance is 1.95 Å which is quite different from 2.06 Å calculated based on our experimental data and those reported in refs *30, 36, 56–59*. Despite these differences, all the cited studies confirm that the average $Cu-O$ distances are shorter in $Cu^{2+}-HS$ complexes than in either aqua or salicylate systems, while the axial distortion is suppressed. In all cases, the CuO_6 octahedral model permits the experimental data to be fit reasonably well, while the inclusion of atoms other than oxygen into the inner complexation shell is not warranted.

In our experiments with $Cu^{2+}-HS$ systems, the contribution of atoms beyond the first complexation shell to the FT magnitude was not well defined (Figure 5A). This was caused by highly disordered distributions of the distant atoms in solutions. The EXAFS analysis procedure used in our calculations is applicable only to systems with small to moderate disorder for which the quasi-Gaussian model is a good approximation for the unknown radial pair distribution function $\rho(r)$. When the structural disorder is large, the approximation of the $\rho(r)$ by a rapidly converging series of cumulants is incorrect. Though specific EXAFS analysis techniques have been developed for strongly disordered systems (*34*), their applicability is limited to structures formed by well separated shells of identical atoms which is certainly not the case for $Cu^{2+}-HS$ complexes. On the basis of the lack of prominent and easily distinguishable features in the FT magnitudes of $Cu^{2+}-HS$ complexes at $r > 2.5$ Å, it is concluded that by using the EXAFS method only it is unlikely to unambiguously determine the nature and structural properties of the atoms lying beyond the first complexation shell for metal–HS complexes. The performance of EXAFS

in combination with other structure-sensitive methods deserves to be explored in more detail.

Literature Cited

(1) McIntyre, C.; Batts, B. D.; Jardine. D. R. *J. Mass Spectrom.* **1997**, *32*, 328.
(2) Remmler, M.; Georgi, A.; Kopinke, F.-D. *Eur. J. Mass Spectrom.* **1995**, *22*, 403.
(3) Gjessing, E. T. *Physical and Chemical Characterisitcs of Aquatic Humus*; Ann Arbor Science: Ann Arbor, MI, 1976.
(4) Ghosh, K.; Schnitzer, M. *Soil Sci.* **1980**, *129*, 266.
(5) Schulten, H.-R.; Schnitzer, M. *Sci. Total Environ.* **1992**, *117/118*, 27.
(6) Leenheer, J. A.; Wilson, M. A.; Malcolm, R. L. *Org. Geochem.* **1987**, *11*, 273.
(7) Barancikova, G.; Senesi, N.; Brunetti, G. *Geoderma* **1997**, *78*, 251.
(8) Kiss, T.; Micera, G.; Sanna, D.; Kozlowski, H. *J. Chem. Soc., Dalton Trans.* **1994**, No. 3, 347.
(9) Hess, A. N.; Chin, Y. P. *Colloids Surf.* **1996**, *107*, 141.
(10) Ricca, G.; Severini, F. *Geoderma* **1993**, *58*, 233.
(11) Edwards, M.; Benjamin, M. M.; Ryan, J. N. *Colloids Surf.* **1996**, *107*, 297.
(12) Leenheer, J. A.; Wershaw, R. L.; Reddy, M. M. *Environ. Sci. Technol.* **1995**, *29*, 399.
(13) Bailey, G. W.; Shevchenko, S. M.; Kamermans, H. *J. Soil Sci. Soc. Am.* **1997**, *61*, 92.
(14) Pompe, S.; Bubner, M.; Denecke, M. A.; Reich, T.; Brachmann, A.; Geipel, G.; Nicolai, R.; Heise, K. H.; Nitsche, H. *Radiochim. Acta* **1996**, *74*, 135.
(15) Bavoso, A.; Menabue, L.; Saladini, M.; Sola, M. *Inorg. Chim. Acta* **1996**, *244*, 207.
(16) Ikan, R.; Ioselis, P.; et al. *Sci. Total Environ.* **1992**, *117/118*, 1.
(17) Lu, X. Q.; Johnson, W. D. *Sci. Total Environ.* **1997**, *203*, 199.
(18) Breault, R. F.; Colman, J. A.; Aiken, G. R.; McKnight, D. *Environ. Sci. Technol.* **1996**, *30*, 3477.
(19) Luster, J.; Lloyd, T.; Sposito, G. *Environ. Sci. Technol.* **1996**, *30*, 1565.
(20) Ephraim, J. H.; Marinsky, J. A. *Anal. Chim. Acta* **1990**, *232*, 171.
(21) Ephraim, J. H.; Marinsky, J. A. *Environ. Sci. Technol.* **1986**, *20*, 367.
(22) Cabaniss, S. E.; Shuman, M. S. *Geochim. Cosmochim. Acta* **1988**, *52*, 185.
(23) Gamble, D. S.; Langford, C. H.; Underdown, A. W. *Org. Geochem.* **1985**, *8*, 35.
(24) Saar, R. A.; Weber, J. H. *Anal. Chem.* **1980**, *52*, 2095.
(25) Buffle, J.; Greter, F.-L.; Haerdi, W. *Anal. Chem.* **1977**, *49*, 216.
(26) Stevenson, F. J. *Soil Sci.* **1977**, *123*, 10.
(27) Guy, R. D.; Charkrabarti, C. L. *Can. J. Chem.* **1976**, *54*, 2600.
(28) Wilson, D. E.; Kinney, P. *Limnol. Oceanogr.* **1977**, *22*, 281.
(29) Linder, P. W.; Murray, K. *Sci. Total Environ.* **1987**, *64*, 149.
(30) *X-ray diffraction of ions in aqueous solutions: hydration and complex formation*; Magini, M., Ed.; CRC Press: Boca Raton, FL, 1988.
(31) Stern, E. A.; Heald, S. M. In *Handbook on Synchrotron Radiation*; Koch, E. E., Ed.; North-Holland: Amsterdam, 1983.
(32) Stern, E. A.; Newville, M.; Ravel, B.; Yacoby, Y.; Haskel, D. *Phys. B* **1995**, *208/209*, 117.
(33) Zabinsky, S. I.; Rehr, J. J.; Ankudinov, A.; Albers, R. C.; Eller, M. J. *Phys. Rev. B* **1995**, *52*, 2995.

(34) *X-ray absorption: principles, applications, techniques of EXAFS, SEXAFS, and XANES*; Koningsberger, D. C., Prins, R., Eds.; Wiley: New York, 1988.

(35) Moller, K.; van Etten, R. L. *Biospectroscopy* **1997**, *3*, 85.

(36) Inada, Y.; Ozutsumi, K.; Funabashi, S.; Soyama, S.; Kawashima, T.; Tanaka, M. *Inorg. Chem.* **1993**, *32*, 3010.

(37) Hersterberg, D.; Sayers, D. E.; Zhou, W.; Robarge, W. P.; Plummer, G. M. *J. Phys. IV France* **1997**, *7*, C2−833.

(38) Sarret, G.; Manceau, A.; Hazelman, I. L.; Gomez, A.; Mench, M. *J. Phys. IV France* **1997**, *7*, C2−799.

(39) Helz, G. R.; Miller, C. V.; Charnock, J. M.; Mosselmans, J. F. W.; Pattrick, R. A. D.; Garner, C. D.; Vaughan, D. J. *Geochim. Cosmochim. Acta* **1996**, *60*, 3631.

(40) Xia, K.; Bleam, W.; Helmke, P. A. *Geochim. Cosmochim. Acta* **1997**, *61*, 2211.

(41) Xia, K.; Bleam, W.; Helmke, P. A. *Geochim. Cosmochim. Acta* **1997**, *61*, 2223.

(42) Leenheer, J. A. *Environ. Sci. Technol.* **1981**, *15*, 578.

(43) Korshin, G. V.; Benjamin, M. M.; Sletten, R. S. *Water Res.* **1997**, *31*, 1643.

(44) Chang, Y. J.; Li, C. W.; Benjamin, M. M. *J. Am. Water Works Assoc.* **1997**, *89*, no. 5, 100.

(45) Schecher, W. D.; McAvoy, D. C. *MINEQL+: A Chemical Equilibrium Software;* Hollowell, Md.: Environmental Research Software, 1994.

(46) Stern, E. A.; Heald, S. M. *Rev. Sci. Instrum.* **1979**, *50*, 1579.

(47) Sayers, D. A.; Stern, E. A.; Lytle, F. W. *Phys. Rev. Lett.* **1971**, *27*, 1204.

(48) Stern, E. A.; Sayers, D. A.; Lytle, F. W. *Phys. Rev. B* **1975**, *11*, 4836.

(49) Newville, M.; Livins, P.; Yacoby, Y.; Rehr, J. J.; Stern, E. A. *Phys. Rev. B* **1993**, *47*, 14126.

(50) Frenkel, A. I.; Stern, E. A.; Qian, M.; Newville, M. *Phys. Rev. B* **1993**, *48*, 12449.

(51) Frenkel, A. I.; Stern, E. A.; Voronel, A.; Qian, M.; Newville, M. *Phys. Rev. Lett.* **1993**, *71*, 3485.

(52) Stern, E. A. *Phys. Rev. B* **1993**, *48*, 9825.

(53) Palladino, L.; Della Longa, S.; Reale, A.; Belli, M.; Scafatti, S.; Onori, G.; Santucci, A. *J. Chem. Phys.* **1993**, *98*, 2720.

(54) Garcia, J.; Benfatto, M.; Natoli, C. R.; Bianconi, A.; Fontaine, A.; Tolentino, H. *Chem. Phys.* **1989**, *132*, 295.

(55) Kuznetsov, An. M.; Korshin, G. V.; Frenkel, A. I.; Masliy, A. N. Manuscript in preparation.

(56) D'Angelo, P.; Bottari, E.; Festa, M. R.; Nolting, H.-F.; Pavel, N. V. *J. Chem. Phys.* **1997**, *107*, 2807.

(57) Inada, Y.; Sugimoto, K.; Ozutsumi, K.; Funabashi, S. *Inorg. Chem.* **1994**, *33*, 1875.

(58) Ozutsumi, K.; Kawashima, T. *Polyhedron* **1992**, *11*, 169.

(59) Ozutsumi, K.; Miyata, Y.; Kawashima, T. *J. Inorg. Biochem.* **1991**, *44*, 97.

(60) Morra, J. M.; Fendorf, S. E.; Brown, P. D. *Geochim. Cosmochim. Acta* **1997**, *61*, 683.